


Geodesic intersections

Charles F. F. Karney *

SRI International, 201 Washington Rd, Princeton, NJ 08540-6449, USA

(Dated: December 20, 2023)

A complete treatment of the intersections of two geodesics on the surface of an ellipsoid of revolution is given. With a suitable metric for the distances between intersections, bounds are placed on their spacing. This leads to fast and reliable algorithms for finding the closest intersection, determining whether and where two geodesic segments intersect, finding the next closest intersection to a given intersection, and listing all nearby intersections. The cases where the two geodesics overlap are also treated.

1. INTRODUCTION

In this paper, I provide a method for finding the intersection of two geodesics on the surface of an ellipsoid of revolution. This elaborates on the method given by Baselga and Martínez-Llario (2018, henceforth referred to as *BML*) in two regards. Firstly I correct their formulation of the solution of the intersection problem for a sphere. Secondly, I ensure that the *closest* intersection is found.

The intersection problem was previously tackled by Sjöberg (2008); however, he makes the problem unnecessarily complicated by combining the solution of the geodesic problem and finding the intersection. In contrast, *BML* assume the solution of the inverse geodesic problem is given by Karney (2013). In §8 of this latter paper, I also provided a solution to the intersection problem using the ellipsoidal gnomonic projection; however, although this projection is useful in converting various geodesic problems to equivalent problems in plane geometry, it is restricted to cases where the intersection is sufficiently close.

The outline of the method given here is as follows. In the first instance, a geodesic is specified by its position (latitude and longitude, ϕ_0 and λ_0) and azimuth α_0 and we establish a criterion for the “closest” intersection of two such geodesics. I use the method of *BML*, with fixes given in Appendix A, to determine a “nearby” intersection. In a minority of cases, the resulting intersection is not the closest and a search needs to be made for alternate intersections, and the closest one is then picked. Finally, we consider variants:

- Find the intersection of two geodesic segments, specified by their endpoints.
- Given a particular intersection, find the next closest intersection.
- List all the intersections within a certain distance.

We treat here ellipsoids of revolution with equatorial radius a and polar semi-axis b . The shape of the ellipsoid is parameterized by the flattening $f = (a - b)/a$, the third flattening $n = (a - b)/(a + b)$, or the eccentricity $e = \sqrt{a^2 - b^2}/a$.

The main application for this method is terrestrial ellipsoids for which $f \approx \frac{1}{300}$. However, if we restrict our attention to such ellipsoids, we might overlook some ellipsoidal effects. To avoid this, we consider ellipsoids with third flattening satisfying $|n| \leq 0.12$; this includes the range of flattenings $-\frac{1}{4} \leq f \leq \frac{1}{5}$ which corresponds to $\frac{4}{5} \leq b/a \leq \frac{5}{4}$. (The methods can be applied to Saturn with $f \approx \frac{1}{10}$.) We then expect to contend with the same effects as terrestrial ellipsoids, just in an exaggerated form. We intentionally do not treat more extreme flattenings which may introduce qualitatively new behavior.

Because the range of flattenings considered exceeds the limit $|f| \leq \frac{1}{50}$ of validity for the series approximations for geodesics given in Karney (2013), we shall also use the formulation for geodesics in terms of elliptic integrals described in Karney (2022). When applying the methods to terrestrial ellipsoids, the simpler series solution can be used.

2. POSING THE PROBLEM

A geodesic X on an ellipsoid can be specified by its starting position $(\phi_{x0}, \lambda_{x0})$ and azimuth α_{x0} . Traveling a signed displacement x from the starting point gives a position (ϕ_x, λ_x) and azimuth α_x . If we consider two such geodesics X and Y , then an intersection is given by the pair of displacements $\mathbf{S} = [x, y]$ for which the geodesic distance between (ϕ_x, λ_x) and (ϕ_y, λ_y) vanishes.

This investigation starts with the solution to the intersection problem given by *BML*. The method involved repeatedly solving a spherical triangle given an edge and its two adjacent angles; this provides an iterative method of determining *an* intersection. Appendix A outlines this method and includes recasting the algorithm to ensure that it always converges and that, for the sphere, it gives the closest intersection. This “basic algorithm” maps a tentative intersection \mathbf{S} (which might be the origin $\mathbf{0}$, where the geodesics are specified) to some nearby intersection $\mathbf{b}(\mathbf{S})$.

BML suggest using the equatorial radius a as the equivalent radius for the sphere. However, a better choice for this method is $R = \langle K \rangle^{-1/2}$, where K is the Gaussian curvature and the average is over the surface of the ellipsoid. The Gaussian curvature is the appropriate curvature for this application because this describes the intrinsic properties of the surface regardless of how it is embedded in three-dimensional space. For any surface with the topology of a ball, the Gauss-Bonnet theorem

*Email addresses: charles.karney@sri.com; karney@alum.mit.edu.

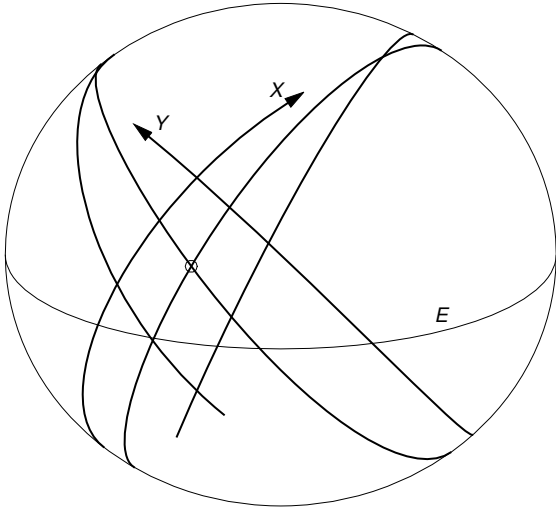


FIG. 1 Intersections of two geodesics X and Y on an ellipsoid with flattening $f = \frac{1}{10}$. This shows an orthographic view of the geodesics on the ellipsoid; the geodesics start at a point with latitude $\phi_{x0,y0} = 20^\circ$, longitude $\lambda_{x0,y0} = 0^\circ$ marked with a circle with azimuths $\alpha_{x0} = 25^\circ$ and $\alpha_{y0} = -45^\circ$ and are followed somewhat more than one complete circuit of the ellipsoid in each direction. The equator is labeled E .

gives

$$\int K \, dA = 4\pi, \quad (1)$$

where dA is an area element and the integral is over the surface of the ellipsoid. Dividing this by

$$\int dA = A, \quad (2)$$

the total area, we obtain $\langle K \rangle = 4\pi/A$; this then establishes that $A = 4\pi R^2$, i.e., that R is the authalic radius. For an ellipsoid of revolution, we have

$$R = \sqrt{\frac{a^2}{2} + \frac{b^2 \tanh^{-1} e}{e}}. \quad (3)$$

In the remainder of this paper, we set $R = 1/\pi$ so that the circumference of the authalic sphere is 2. (Alternatively, the reader can understand that all lengths are in units of πR .)

Next, let us consider how to define the closest intersection. For this we need a measure of distance in $\mathbf{S} = [x, y]$ space and plausible choices are the L_1 distance,

$$L_1(\mathbf{S}) = |x| + |y|, \quad (4)$$

and the L_∞ distance,

$$L_\infty(\mathbf{S}) = \max(|x|, |y|). \quad (5)$$

(The familiar L_2 distance, $L_2(\mathbf{S}) = \sqrt{x^2 + y^2}$ makes no sense in this context because \mathbf{S} is not a Euclidean space.) As we

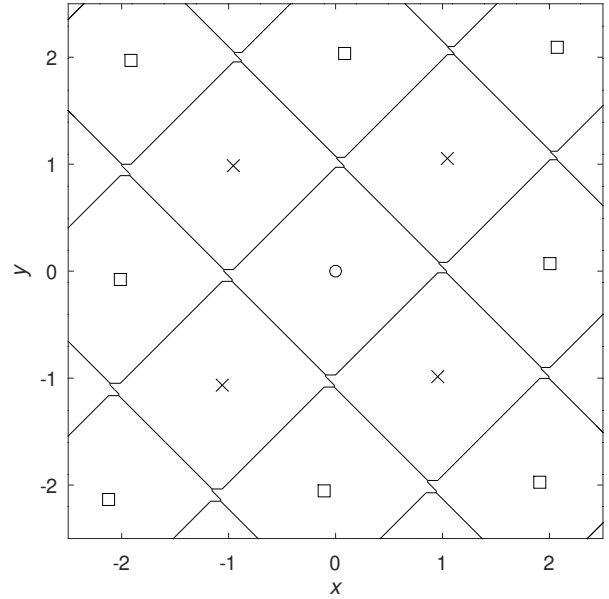


FIG. 2 The geodesic intersections shown in Fig. 1 laid out in the $\mathbf{S} = [x, y]$ plane, where x and y are the displacements along the two geodesics; the starting point is labeled with a circle; the other 8 intersections visible in Fig. 1 are labeled with squares; and crosses label the 4 intersections on the opposite side of the ellipsoid. The lines give the L_1 Voronoi partition.

shall see, the L_1 distance aligns better with the way geodesics behave and we shall adopt this way of determining closeness. We therefore use the simpler notation

$$|\mathbf{S}| = L_1(\mathbf{S}). \quad (6)$$

\mathbf{S} is a vector space so the distance between two points $\mathbf{S}_1 = [x_1, y_1]$ and $\mathbf{S}_2 = [x_2, y_2]$ is just $|\mathbf{S}_2 - \mathbf{S}_1|$. We define $\mathbf{c}(\mathbf{S})$ as the intersection that is closest to \mathbf{S} ; i.e., it minimizes $|\mathbf{c}(\mathbf{S}) - \mathbf{S}|$.

For a sphere, geodesics reduce to great circles that repeatedly intersect at two antipodal points. The situation is more complex on an ellipsoid because geodesics are not, in general, closed curves, so they repeatedly intersect at different points on the ellipsoid. (For now, we exclude the case of overlapping geodesics; this is discussed in Sec. 7.) A typical situation is illustrated in Fig. 1 which shows two geodesics X and Y that start at an intersection, marked with a circle, on an ellipsoid with $f = \frac{1}{10}$.

The intersections are also shown in the $\mathbf{S} = [x, y]$ plane in Fig. 2. \mathbf{S} space is partitioned into regions (shown as lines in the figure) that are closest to the individual intersections; this is just the Voronoi partition defined with the L_1 metric.

Figure 2 would look quite similar for a sphere. In this case, the intersections are located at integer values of x and y such that $x + y$ is even and the L_1 Voronoi partition is a regular tiling by squares oriented at 45° . In fact, in the case of a sphere, the L_2 and L_∞ partitions are identical to the L_1 partition. However, because the partitioned regions are L_1 circles of radius 1 centered at the intersections, the L_1 metric yields tighter bounds on the positions of the intersections and, as a

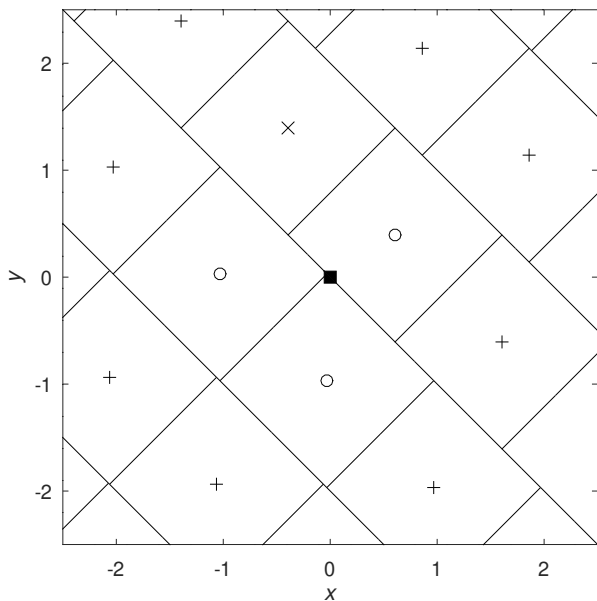


FIG. 3 The Voronoi partition for intersections of two nearly coincident geodesics on an ellipsoid with flattening $f = \frac{1}{297}$. The geodesics are defined by $\phi_{x0} = -50.410^\circ$, $\lambda_{x0} = 0^\circ$, $\alpha_{x0} = -69.179^\circ$, and $\phi_{y0} = 50.411^\circ$, $\lambda_{y0} = 179.863^\circ$, $\alpha_{y0} = 68.835^\circ$. The starting point for the intersection problem is marked by the filled square.

consequence, this metric is the natural choice for defining the closest intersection.

In some cases, the pattern of intersections on an ellipsoid differs markedly from that for a sphere. An example is shown in Fig. 3 where the geodesics are nearly coincident. Here, the points defining the geodesics, namely at $\mathbf{S} = \mathbf{0}$, are approximately antipodal and this causes the intersection found with the basic algorithm method $\mathbf{b}(\mathbf{0})$, shown by a cross in the figure, to be far from the closest. There are three intersections, marked by circles, that are considerably closer. The other intersections are marked with plus signs.

Therefore, we seek to adapt the basic algorithm so that we are guaranteed to find the closest intersection. Henceforth, we will usually drop the L_1 qualifier with the terms, “closest”, “distance”, “radius”, and “circle”, when used in the context of \mathbf{S} space. In this paper, the boldface notation for vectors, e.g., \mathbf{S} and $\mathbf{c}(\mathbf{S})$ is reserved for two-dimensional vectors in the $[x, y]$ plane.

3. BOUNDS ON INTERSECTIONS

A necessary prelude to constructing the solution for the closest intersection is to place limits on intersections. Initially, these limits were found empirically by randomly sampling many (at least 10^6) cases for several values of n satisfying $|n| \leq 0.12$. For each value of n , we can identify the geodesics involved in the limiting cases enabling an accurate determination of the limits.

Let’s start by determining the minimum distance $2t_1$ between intersections. We find that, in the case of an oblate

ellipsoid, the minimum occurs with an intersection given by the nearly equatorial geodesics $\phi_{x0,y0} = 0^\circ$, $\lambda_{x0,y0} = 0^\circ$, $\alpha_{x0,y0} = 90^\circ \pm \epsilon$, for some small ϵ . In the limit $\epsilon \rightarrow 0$, the nearest intersections are at $x = y = \pm\pi b$, i.e., we have $||[x, y]|| = 2\pi b$ and hence $t_1 = \pi b$. This result is expected, because, for an oblate ellipsoid, the maximum curvature occurs at the equator.

This case also illustrates a common trait in these limiting cases, namely that the geodesics are nearly coincident. We postpone a full discussion of such geodesics to Sec. 7. However, it’s possible to find the intersections in these cases by determining where the reduced length m or geodesic scale M of a geodesic is zero. These quantities characterize the behavior of nearby geodesics. Consider a geodesic starting at point 1 and ending at point 2, and a second nearby geodesic starting at the same point but a slightly difference azimuth; the two geodesics intersect at points 2 where $m_{12} = 0$; in these cases, points 1 and 2 are called “conjugate points”. Furthermore, the geodesics are parallel at points 2 where $M_{21} = 0$. Further details are given in Karney (2013, §3); these include expressions for the derivatives of m_{12} and M_{12} which allow the intersections of nearly coincident geodesics to be found by Newton’s method.

The equivalent result for t_1 for a prolate ellipsoid is found by considering a geodesic passing over the pole (where the curvature is maximum). The geodesic, which we denote by p_a should be symmetrically placed over the pole so that $M_{21} = 0$ at the pole. For $n = -0.01$, we find that $\phi_{x0,y0} = \phi_{x,y} = 1.755^\circ$, $\lambda_{x0,y0} = 0^\circ$, $\lambda_{x,y} = 180^\circ$, $\alpha_{x0,y0} = \pm\epsilon$, and $t_1 = p_a = 0.9832$.

The result for the minimum distance between intersections can be summarized by

$$|\mathbf{T}' - \mathbf{T}| \geq 2t_1, \quad (7)$$

where \mathbf{T} and \mathbf{T}' are any two distinct intersections. This result has an important corollary: if \mathbf{T} is an intersection satisfying $|\mathbf{T}| < t_1$ then it is the closest intersection to $\mathbf{0}$, i.e., $\mathbf{T} = \mathbf{c}(\mathbf{0})$. This is proved by considering the distance to some other intersection $|\mathbf{T}'|$ which is constrained by the triangle inequality,

$$|\mathbf{T}'| + |\mathbf{T}| \geq |\mathbf{T}' - \mathbf{T}| \geq 2t_1, \quad (8)$$

or

$$|\mathbf{T}'| \geq 2t_1 - |\mathbf{T}| \geq t_1. \quad (9)$$

Thus \mathbf{T} is closer than \mathbf{T}' , provided that $|\mathbf{T}| < t_1$.

We next place an upper limit on the distance to the closest intersection. Let \mathbf{T} be the intersection closest to $\mathbf{0}$, then $|\mathbf{T}| \leq t_2$. The empirical results indicate that t_2 is given by switching the results for t_1 for oblate and prolate ellipsoids giving $t_2 = p_a$ for oblate ellipsoids and $t_2 = \pi b$ for prolate ellipsoids. Again this result makes sense since the corresponding geodesics are now sampling regions of minimum curvature on the ellipsoid.

The result for the nearest intersection to a given intersection is

$$|\mathbf{T}' - \mathbf{T}| \leq 2t_3. \quad (10)$$

For prolate ellipsoids, we find that $t_3 = 2Q$, where Q is the length of the quarter meridian; $2t_3$ is the L_1 distance

TABLE 1 The special lengths for the intersection problem of a sphere and oblate ellipsoids, $n \geq 0$; the authalic radius is taken to be $R = 1/\pi$. The quantities a and b are the equatorial radius and the polar semi-axis; Q is the quarter meridian distance. The other quantities p_a , p_b , o_c , and t_1 thru t_5 are defined in the text.

n	πa	πb t_1, t_4	$2Q$ t_5	p_a t_2	p_b	o_c t_3
0	1	1	1	1	1	1
0.01	1.0067	0.9867	0.9967	1.0165	1.0230	1.0017
0.02	1.0133	0.9735	0.9935	1.0328	1.0463	1.0034
0.03	1.0199	0.9605	0.9904	1.0487	1.0698	1.0052
0.04	1.0264	0.9475	0.9874	1.0644	1.0935	1.0071
0.05	1.0330	0.9346	0.9844	1.0796	1.1175	1.0090
0.06	1.0395	0.9218	0.9815	1.0944	1.1417	1.0110
0.07	1.0460	0.9091	0.9788	1.1088	1.1661	1.0131
0.08	1.0524	0.8965	0.9760	1.1227	1.1906	1.0153
0.09	1.0589	0.8840	0.9734	1.1361	1.2153	1.0175
0.10	1.0652	0.8716	0.9708	1.1490	1.2402	1.0198
0.11	1.0716	0.8592	0.9683	1.1613	1.2651	1.0222
0.12	1.0779	0.8469	0.9659	1.1732	1.2901	1.0246

between an intersection of two meridians at one pole and the intersection at the opposite pole. The oblate ellipsoids, the limiting geodesics are oblique (labeled o_c) and are given by an intersection on the equator with two nearby azimuths approximately equal to 45° with the azimuth adjusted so that there are 6 equally distant nearest intersections. For $n = 0.01$, this is achieved with $\phi_{x0,y0} = 0^\circ$, $\lambda_{x0,y0} = 0^\circ$, $\alpha_{x0,y0} = 45.062^\circ \pm \epsilon$, with nearest intersections at $[\pm o_c, \pm o_c]$, $[\pm 1.4976, \mp 0.5058]$, and $[\pm 0.5058, \mp 1.4976]$, where $t_3 = o_c = 1.0017 = \frac{1}{2}(1.4976 + 0.5058)$.

Next, we determine the ‘‘capture radius’’ t_4 of the basic algorithm. If \mathbf{T} is an intersection that satisfies

$$|\mathbf{T} - \mathbf{S}| < t_4, \quad (11)$$

where \mathbf{S} is an arbitrary point, then

$$\mathbf{T} = \mathbf{b}(\mathbf{S}) = \mathbf{c}(\mathbf{S}). \quad (12)$$

In other words, the basic algorithm applied at \mathbf{S} is guaranteed to return the closest intersection provided it is within a radius t_4 of \mathbf{S} .

The basic algorithm switches between neighboring intersections when $\mu_y - \mu_x = 0$ or π in Fig. 7. For z small, this is the condition that the geodesics are parallel, and this, in turn, is given by $M_{21} = 0$ for a geodesic starting at an intersection. As in the determination of t_1 , the limiting case is given when the geodesics lie in the region of maximum curvature. For an oblate ellipsoid, we have $t_4 = t_1 = \pi b$. For a prolate ellipsoid, it is again a geodesic passing over the pole, but this time asymmetrically; we denote this geodesic by p_b . For $n = -0.01$, we start at an intersection $\phi_{x0,y0} = 26.783^\circ$, $\lambda_{x0,y0} = 0^\circ$, $\alpha_{x0,y0} = \pm \epsilon$ and the condition $M_{21} = 0$ is obtained at $x = y = \frac{1}{2}p_b$, $\phi_{x,y} = 64.192^\circ$, and $\lambda_{x,y} = 180^\circ$. The distance from this point to the intersection is $t_4 = p_b = 0.9773$.

TABLE 2 The parameters listed in Table 1 computed for prolate ellipsoids, $n < 0$. The first row of headings match those in Table 1; however the pairing of these with t_1 thru t_5 listed in the second row of headings is different.

n	πa	πb t_2	$2Q$ t_5, t_3	p_a t_1	p_b t_4	o_c
-0.01	0.9933	1.0134	1.0034	0.9832	0.9773	0.9984
-0.02	0.9866	1.0269	1.0068	0.9662	0.9549	0.9967
-0.03	0.9799	1.0405	1.0104	0.9491	0.9327	0.9952
-0.04	0.9731	1.0542	1.0141	0.9317	0.9109	0.9936
-0.05	0.9663	1.0681	1.0178	0.9143	0.8893	0.9920
-0.06	0.9595	1.0820	1.0217	0.8968	0.8681	0.9905
-0.07	0.9527	1.0961	1.0257	0.8792	0.8472	0.9889
-0.08	0.9459	1.1103	1.0297	0.8616	0.8266	0.9873
-0.09	0.9390	1.1247	1.0339	0.8440	0.8064	0.9856
-0.10	0.9321	1.1392	1.0382	0.8265	0.7864	0.9839
-0.11	0.9251	1.1538	1.0426	0.8089	0.7668	0.9822
-0.12	0.9182	1.1686	1.0472	0.7914	0.7475	0.9803

When finding the intersection of geodesic segments, we require the maximum length of a shortest geodesic segment, t_5 . This is just the distance between the poles, twice the quarter meridian distance, i.e., $t_5 = 2Q$.

These lengths are tabulated in Table 1 for oblate ellipsoids with $0 \leq n \leq 0.12$ and Table 2 for prolate ellipsoids with $-0.12 \leq n < 0$. The first row of headings reflects where on the ellipsoid the geodesics lie. In contrast, the second row lists the relationship with the distances t_1 thru t_5 . The ratios of the distances a , b , R , Q can be found by elementary means (for Q , this entails solving the inverse geodesic problem between a pole and a point on the equator). The distances p_a , p_b , and o_c are found using iterative methods; code for these calculations is provided in the constructor for the `Intersect` class in the implementation described in Sec. 8. However, the algorithms do not depend on the exact values of t_1 thru t_5 . The algorithms given below will ‘‘work’’ (albeit slightly less efficiently) if the quantities are replaced by their values at a larger value of $|n|$.

4. FINDING THE CLOSEST INTERSECTION

We are now in a position to consider the problem of finding the closest intersection. The lengths t_1 thru t_4 found in the previous section are the radii of circles. For example, the definition of t_2 can be reformulated by saying that the closest intersection is inside a circle of radius t_2 . Now L_1 circles have the property that a circle of radius s can be exactly tiled by m^2 circles of radius s/m . Thus the basic algorithm can find *all* the intersections in the circle of radius t_2 by running it with four starting points $\{[\pm d_1, 0], [0, \pm d_1]\}$, where $d_1 = \frac{1}{2}t_2$. For $|n| \leq 0.12$, we then have $d_1 < t_4$ and each application of the basic algorithm is guaranteed to find any intersections within a quarter of the circle of radius t_2 ; furthermore, there is at least one intersection within this circle. All that remains is to pick the intersection closest to $\mathbf{0}$.

We can optimize this procedure by observing that for any intersection \mathbf{T} :

- If $|\mathbf{T}| < t_1$, then \mathbf{T} is the intersection closest to $\mathbf{0}$, $\mathbf{c}(\mathbf{0})$.
- Otherwise, the closest intersection is either \mathbf{T} or is an intersection \mathbf{T}' where $|\mathbf{T}' - \mathbf{T}| \geq 2t_1$.

The first of these suggests that we start with an application of $\mathbf{b}(\mathbf{0})$, and the second lets us remove certain of the remaining starting points as the method progresses.

The algorithm for the closest intersection $\mathbf{c}(\mathbf{0})$ is then

1. Set $\mathbf{T} = [\infty, \infty]$, $d_1 = \frac{1}{2}t_2$, $\delta = \sqrt[3]{\epsilon}$ ($\epsilon = 2^{-52}$ for double-precision arithmetic), $m = 5$, and \mathbf{S}_i for $0 \leq i < m$ to the set of m starting points, $\{\mathbf{0}, [\pm d_1, 0], [0, \pm d_1]\}$. Also set $e_i = \text{false}$ for $0 \leq i < m$; these are “exclusion flags” with $e_i = \text{true}$ indicating that the starting point \mathbf{S}_i can be skipped.
2. For each i satisfying $0 \leq i < m$ and $\neg e_i$ do:
 - (a) Apply the basic algorithm method starting at \mathbf{S}_i , setting $\mathbf{T}_i = \mathbf{b}(\mathbf{S}_i)$.
 - (b) If $|\mathbf{T}_i| < t_1$, set $\mathbf{T} = \mathbf{T}_i$ and go to step 3.
 - (c) If $|\mathbf{T}_i| < |\mathbf{T}|$, set $\mathbf{T} = \mathbf{T}_i$.
 - (d) For each j satisfying $i < j < m$ and $\neg e_j$, set $e_j = (|\mathbf{T}_i - \mathbf{S}_j| < 2t_1 - d_1 - \delta)$.
3. Return \mathbf{T} as the closest intersection, $\mathbf{c}(\mathbf{0})$.

Figure 4 illustrates this algorithm in action. Figure 4(a) shows the first application of the basic algorithm, Step 2(a) for $i = 0$, gives the intersection \mathbf{T}_0 . A labels the circle of radius t_2 inside which the closest intersection must lie, and B labels the circle of radius t_1 inside which any intersection is guaranteed to be the closest. \mathbf{T}_0 lies inside A and outside B (the test in Step 2(b) fails) and so all we know is that it *may* be the closest intersection. The algorithm then repeats the basic algorithm at points \mathbf{S}_i for $i = 1$ thru 4. Each application is responsible for finding intersections in a circle of radius $d_1 = \frac{1}{2}t_2$ centered at \mathbf{S}_i ; this divides the circle A into 4 equal pieces delineated by dashed lines; see Fig. 4(b). However, the presence of the intersection at \mathbf{T}_0 means that there can be no intersection within the “exclusion” circle of radius $2t_1$ centered at \mathbf{T}_0 , labeled E_0 and shown as a dot-dashed line; because this encompasses the circles allotted to \mathbf{S}_2 and \mathbf{S}_4 , we can skip the application of the basic algorithm for $i = 2$ and 4; this is accomplished by Step 2(d) for $i = 0$. The second application of the basic algorithm, $i = 1$, finds \mathbf{T}_1 which is closer than \mathbf{T}_0 , Step 2(c); see Fig. 4(c). The exclusion circle (labeled E_1) centered at \mathbf{T}_1 encompasses the circle allotted to \mathbf{S}_3 . We therefore can skip the remaining iterations and the algorithm terminates with \mathbf{T}_1 as the closest intersection.

Even though an application of the basic algorithm at \mathbf{S}_i can capture intersections within a circle of radius t_4 , we nevertheless assign it “responsibility” for a *smaller* circle of radius d_1 . This allows more iterations to be skipped on account of Step 2(d). Finally, the test in Step 2(d) includes a “safety margin” δ ; this ensures that the exclusions don’t result in missing intersections lying *on* the boundaries of the circles of radius d_1 in Fig. 4(b).

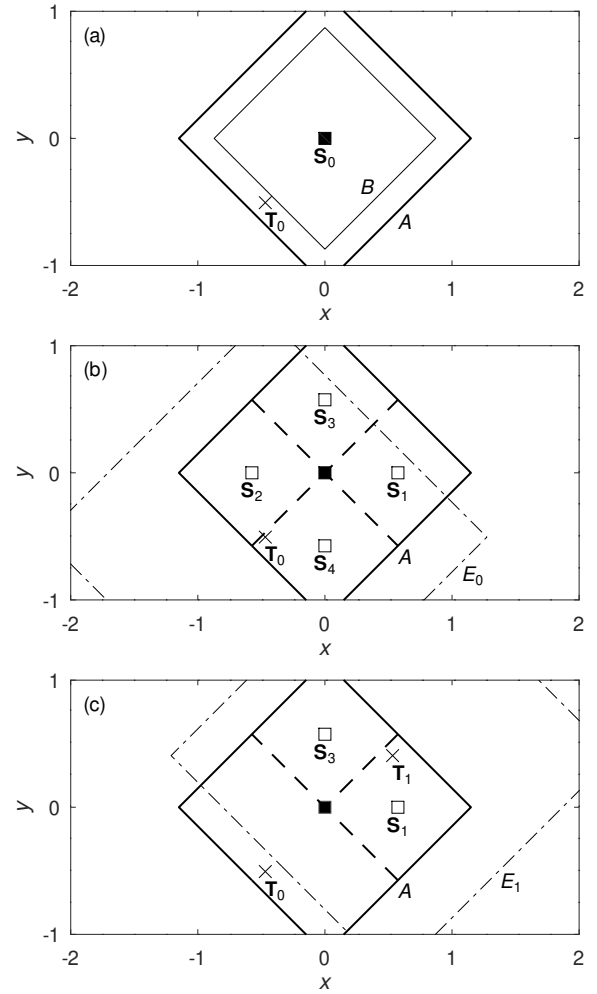


FIG. 4 An example of finding the closest intersection. Here we take $n = \frac{1}{10}$, $\phi_{x0} = 36.873^\circ$, $\lambda_{x0} = 0^\circ$, $\alpha_{x0} = 60.641^\circ$, and $\phi_{y0} = -62.631^\circ$, $\lambda_{y0} = 75.301^\circ$, $\alpha_{y0} = 30.776^\circ$. Parts (a), (b), and (c) illustrate successive stages in the algorithm, as explained in the text.

5. THE INTERSECTION OF TWO GEODESIC SEGMENTS

A common application for intersections is finding if and where two geodesic segments X and Y intersect. Each segment is specified by its endpoints, e.g., $(\phi_{x1}, \lambda_{x1})$ and $(\phi_{x2}, \lambda_{x2})$ and we stipulate that there’s a unique shortest geodesic connecting each pair of endpoints. As a consequence, the two segments intersect at most once. Displacements along the geodesic are measured from the first endpoint, positive towards the second endpoint. Let s_x and s_y be the lengths of the segments; then the segments intersect provided that the intersection is within the $s_x \times s_y$ rectangle H specified by $0 \leq x \leq s_x$ and $0 \leq y \leq s_y$.

We start by applying the algorithm for the closest intersection to the midpoint $\mathbf{M} = \frac{1}{2}[s_x, s_y]$, i.e., we compute $\mathbf{T}_0 = \mathbf{c}(\mathbf{M})$. If \mathbf{T}_0 is within H , then the segments intersect at \mathbf{T}_0 and we’re done.

Otherwise, we need to check whether there’s some other intersection within H . Now \mathbf{T}_0 is the closest intersection to \mathbf{M} . But there may be a more distant intersection lying near the

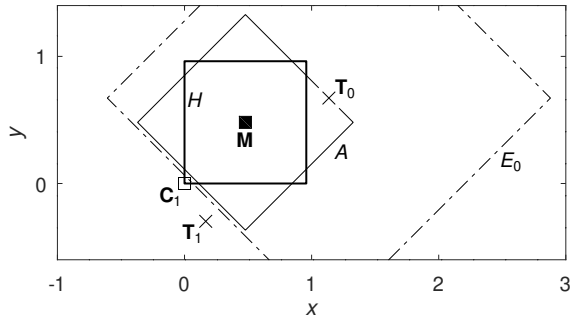


FIG. 5 An illustration of segment intersection with $n = \frac{1}{10}$, $\phi_{x1} = -56.739^\circ$, $\lambda_{x1} = 0^\circ$, $\phi_{x2} = 54.809^\circ$, $\lambda_{x2} = -175.812^\circ$, and $\phi_{y1} = -33.312^\circ$, $\lambda_{y1} = -67.388^\circ$, $\phi_{y2} = 34.788^\circ$, $\lambda_{y2} = 117.255^\circ$.

corners of H ; this requires

$$\frac{1}{2}(s_x + s_y) \geq |\mathbf{T}_0 - \mathbf{M}|. \quad (13)$$

If this inequality holds, consider each corner \mathbf{C}_i ($0 < i \leq 4$) of the intersection rectangle, $\{[0, 0], [s_x, 0], [0, s_y], [s_x, s_y]\}$; if \mathbf{C}_i lies outside the exclusion radius for \mathbf{T}_0 , i.e., if

$$|\mathbf{T}_0 - \mathbf{C}_i| \geq 2t_1, \quad (14)$$

then we apply the basic algorithm and compute $\mathbf{T}_i = \mathbf{b}(\mathbf{C}_i)$; if \mathbf{T}_i lies within H , we accept \mathbf{T}_i as the result. The procedure is illustrated in Fig. 5, where the segment rectangle H is shown with a heavy line. First, the intersection closest to the midpoint \mathbf{M} , the solid square, is found giving $\mathbf{T}_0 = \mathbf{c}(\mathbf{M})$. Because the corners of H are further from \mathbf{M} than \mathbf{T}_0 (outside the circle A), we check for intersections close to the corners. Only one corner \mathbf{C}_1 , marked with an open square, lies outside the exclusion circle E_0 of radius $2t_1$ centered at \mathbf{T}_0 , shown with a dot-dashed line. An application of the basic algorithm yields the intersection $\mathbf{T}_1 = \mathbf{b}(\mathbf{C}_1)$. Since this is outside H , the segments do not intersect (and \mathbf{T}_0 is returned as the closest intersection for the segments).

It turns out that we hardly ever have to compute $\mathbf{b}(\mathbf{C}_i)$. Consider the triangle with vertices \mathbf{M} , \mathbf{T}_0 , and \mathbf{C}_i (for some i). The triangle inequality states that

$$|\mathbf{C}_i - \mathbf{M}| \geq |\mathbf{T}_0 - \mathbf{C}_i| - |\mathbf{T}_0 - \mathbf{M}|. \quad (15)$$

Rewriting Eq. (13) as

$$|\mathbf{C}_i - \mathbf{M}| \geq |\mathbf{T}_0 - \mathbf{M}|, \quad (16)$$

and adding this to Eq. (15) gives

$$2|\mathbf{C}_i - \mathbf{M}| \geq |\mathbf{T}_0 - \mathbf{C}_i|. \quad (17)$$

Finally substituting Eq. (14) and $|\mathbf{C}_i - \mathbf{M}| = \frac{1}{2}(s_x + s_y)$, we obtain

$$t_1 \leq \frac{1}{2}(s_x + s_y) < t_5, \quad (18)$$

where the second inequality is just the condition that X and Y are unique shortest geodesics. This represents a fairly narrow range (see Tables 1 and 2) which is satisfied only if the

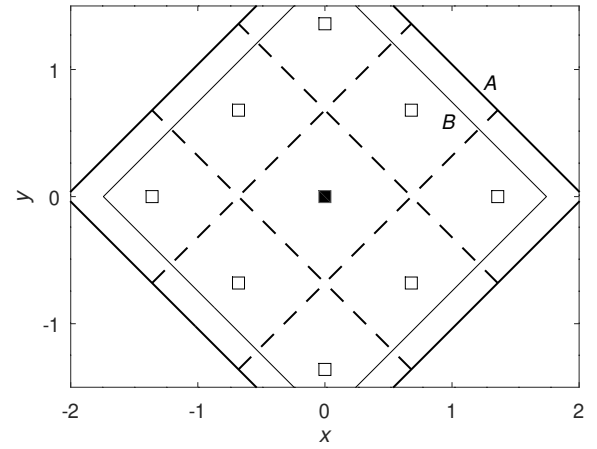


FIG. 6 Finding the next closest intersection to the intersection marked with the filled square. Here, we have $n = \frac{1}{10}$.

endpoints of both X and Y are nearly antipodal. The basic algorithm finds any new intersection near a corner provided that $t_4 > t_5 - t_1$, a condition that holds for $|n| \leq 0.12$.

For uniformly distributed endpoints, the probability that a corner needs to be checked is roughly $1.5 \times f^5$ for small positive f (this is found empirically). Thus the cost of finding the intersection of two segments is only slightly greater than the cost of finding the closest intersection.

A more consequential observation is that I have found *no* cases where \mathbf{T}_i for $i > 0$ yielded a segment intersection that overrode \mathbf{T}_0 . So I conjecture that $\mathbf{c}(\mathbf{M})$ *always* yields the intersection of two segments, provided that they do intersect. If this is true, then the segment intersection algorithm just reduces to the algorithm for the closest intersection.

6. OTHER INTERSECTION PROBLEMS

Our framework can be used to tackle two other intersection problems: finding the next closest intersection to a given intersection and enumerating all the intersections within a certain radius of a starting point.

For the first of these problems, we know the intersection must lie between two concentric circles of radii $2t_3$ and $2t_1$ labeled A and B in Fig. 6. The annular region between these circles can be covered by 8 circles of radius $d_2 = \frac{2}{3}t_3$ (shown with dashed lines), so applications of the basic algorithm starting at the open squares in Fig. 6 will find the next closest intersection provided that $d_2 < t_4$, a condition that holds for $|n| \leq 0.12$. The modifications of the algorithm for the closest intersection given above are: We initialize $m = 8$ and \mathbf{S}_i is the set of m points $\{[\pm 2d_2, 0], [0, \pm 2d_2], [\pm d_2, \pm d_2]\}$. Step 2(b) becomes “If $\mathbf{T}_i = \mathbf{0}$, skip to the next iteration of i .” For the test in Step 2(d), replace d_1 with d_2 .

Three other points: Any tests for equality between intersection points, e.g., $\mathbf{T}' = \mathbf{T}$ should be implemented as $|\mathbf{T}' - \mathbf{T}| < \delta$; remember that intersections can't be arbitrarily close, so if the distance between two intersections is less

than δ the discrepancy is due to roundoff error. A minimum of 8 starting points for the basic algorithm are needed for this particular problem because, in the spherical limit, there are 8 equidistant intersections closest to a given intersection. For terrestrial ellipsoids, nearly equidistant next-closest intersections are reasonably common—so it may be important to check other intersections; this serves as an introduction to the next topic. . .

The last problem we consider is listing all the intersections within some distance D from a starting point. Given the knowledge we’ve already acquired, the solution is straightforward. Divide the circle of radius D evenly into m^2 circles of radius D/m where $m = \lceil D/d_3 \rceil$ and $d_3 = t_4 - \delta$, the capture radius for the basic algorithm reduced by the safety margin. Run the basic algorithm starting at the center of each of the smaller circles and gather up all the distinct intersections lying within D . (We treat intersections closer than δ as being the same; see the previous paragraph.) The optimization in step 2(d) in the algorithm for the closest intersection (replacing d_1 by d_3) should be applied.

7. COINCIDENT GEODESICS

The final topic we consider is coincident geodesics. We touched on this in the specification of the basic algorithm in Appendix A. This returns a flag c which is normally 0 but is set to ± 1 if the geodesics are coincident at the intersection with the sign of c indicating whether the geodesics are parallel or antiparallel.

Let’s consider the application of the basic algorithm that returns an intersection, $\mathbf{T} = [x, y] = \mathbf{b}(\mathbf{S})$, and sets the coincidence flag $c = \pm 1$; then, for arbitrary s , $\mathbf{T}' = [x', y'] = \mathbf{T} + [s, \pm s]$ is also an intersection. When finding the closest intersection, we are interested in the intersection that minimizes the distance from $\mathbf{0}$, i.e., which minimizes $|\mathbf{T}'|$. It’s easy to show graphically that $\min(|\mathbf{T}'|) = |x \mp y|$ and that an interval of s of width $|x \mp y|$ yields this minimum value. Arguably, we could return any value of \mathbf{T}' which gives this value. Nevertheless, it is preferable to pick a definite and predictable value and for this purpose, we pick $s = -\frac{1}{2}(x \pm y)$, for which we have $\mathbf{T}' = \frac{1}{2}[x \mp y, y \mp x]$. This is the value of s that also minimizes the L_∞ distance of \mathbf{T}' from $\mathbf{0}$.

A similar exercise can be carried out for the algorithm for the intersection of segments that coincide. In the cases where the segments overlap, we adjust s to return the intersection in the middle of the overlap region. Otherwise, we return the intersection in the middle of the smallest gap between the segments.

In the case of finding the nearest intersection to a given intersection, we distinguish two cases of coincident intersections

1. An intersection $\mathbf{T} = [x, y]$ is found with $c = \pm 1$, such that $x \mp y = 0$. In this case, the geodesics are coincident at the starting intersection and we treat this as though the geodesics are *nearly* coincident. Therefore, there are intersections at $\mathbf{T}' = [s, \pm s]$ where s is the displacement to successive conjugate points along one of the geodesics given by the condition $m_{12} = 0$.

2. Otherwise, canonicalize the intersection by minimizing the L_∞ distance to $\mathbf{0}$ as we did for finding the closest intersection.

Similar strategies can be used when finding all the intersections. For details, see the implementation.

8. IMPLEMENTATION

The methods described in this paper are included in version 2.3 of GeographicLib (Karney, 2023). The core methods are provided by the C++ class `Intersect`. This can utilize the solution of the geodesic problem in terms of Taylor series (suitable for $|f| \leq \frac{1}{50}$) or elliptic integrals (suitable for any value of f). However, remember that the testing for these methods has been limited to $|n| \leq 0.12$; so this class should not be used for more eccentric ellipsoids. The library also includes a utility, `IntersectTool`, that allows intersections to be computed on the command line.

The routines are optimized by the use of the `GeodesicLine` class. This describes a geodesic specified by a starting point and azimuth. Once this has been set up, computing positions at an arbitrary displacement along the line is about two times faster than solving the direct geodesic problem afresh. The major computational cost is then the solution of the inverse problem in Step 2 of the basic algorithm.

The most useful capabilities are probably finding the closest intersection for two geodesics and finding the intersection of two geodesic segments.

Finding the solution for the closest intersection for randomly chosen geodesics (uniformly distributed positions and azimuths) on the WGS84 ellipsoid, $f = 1/298.257223563$, requires on average 3.16 solutions of the inverse geodesic problem. The first solution found $\mathbf{T}_0 = \mathbf{b}(\mathbf{0})$ is accepted 99.55% of the time in Step 2(b). \mathbf{T}_0 is *eventually* accepted an additional 0.38% of the time, with \mathbf{T}_i for $i > 0$ accepted the remaining 0.07% of the time. If \mathbf{T}_0 is not accepted right away an average of 1.26 additional applications of the basic algorithm are required. The mean number of applications of the basic algorithm is 1.0056.

These results are essentially unchanged for finding the intersection of geodesic segments because, for the WGS84 ellipsoid, the mean number of times the basic algorithm needs to be evaluated at a corner point is minuscule: $1.5 \times f^5 \sim 10^{-12}$. So the cost is then merely that of a closest intersection calculation plus the cost of the two inverse geodesic calculations needed to determine the azimuths for the segments. On a 3.4 GHz Intel processor, the average time to compute the intersection of two segments on the WGS84 ellipsoid is about $12 \mu\text{s}$. The intersection point can be found either by computing the point a displacement x along geodesic X or the point a displacement y along Y . Due to numerical errors, these two computed points do not, in general, coincide; however, they are within about $0.025 \mu\text{m}$ of each other and this is a useful gauge of the overall accuracy of the implementation. The errors in the displacements x and y may be larger than this if the geodesics intersect at a small angle, increasing by about the cosecant of that angle.

9. DISCUSSION

We have given algorithms that reliably find the intersections of geodesics. Our contributions include an important correction to the basic method provided by *BML* followed by a systematic application of this method with selected starting points to obtain the closest intersection and the intersection of geodesic segments.

This allows operations such as computing the union and intersection of polygonal shapes on the surface of an ellipsoid. Coincident geodesics are treated correctly; this is important, for example, in analyzing two polygonal regions that share a boundary.

We offer a conjecture that whenever two geodesic segments intersect, the intersection is the one that is closest to the mid-points of segments.

For terrestrial ellipsoids, the basic method returns the closest intersection in most cases. However, taking the extra steps to ensure that the closest intersection is always returned is crucial: it relieves the user of the library from handling possibly erroneous results and the runtime cost is minimal.

Our treatment applies to moderately eccentric oblate and prolate ellipsoids, $\frac{4}{5} \leq b/a \leq \frac{5}{4}$; we expect similar techniques to apply to more complex surfaces, e.g., a triaxial ellipsoid.

BML also consider the interception problem, namely finding the point on a geodesic closest to some given point. I touch on some aspects of this problem in Appendix B.

10. DATA AVAILABILITY

The source code for the C++ implementation of the intersection routines is available at <https://github.com/geographiclib/geographiclib/tree/r2.3>. This is documented in Karney (2023).

References

- S. Baselga and J. C. Martínez-Llario, 2018, *Intersection and point-to-line solutions for geodesics on the ellipsoid*, Stud. Geophys. Geod., **62**(3), 353–363, doi:10.1007/s11200-017-1020-z.
- V. A. Botnev and S. M. Ustinov, 2015, *Metodika opredeleniya rasstoyaniya mezhdu tochkoy i liniyey v geodezii (Method for finding the distance between a point and a line in geodesy)*, St. Petersburg State Polytechnical University Journal, **6**(234), 33–44, in Russian, <https://infocom.spbstu.ru/en/article/2015.47.4>.
- , 2019, *Metodika opredeleniya rasstoyaniya ot tochki do otrezka v zadachakh navigatsii (Distance finding method between a point and a segment in navigation)*, St. Petersburg State Polytechnical University Journal, **12**(2), 68–79, doi:10.18721/JCSTCS.12206, in Russian.
- C. F. F. Karney, 2013, *Algorithms for geodesics*, J. Geodesy, **87**(1), 43–55, doi:10.1007/s00190-012-0578-z.
- , 2022, *Geodesics on an arbitrary ellipsoid of revolution*, Technical report, SRI International, accepted for publication in J. Geodesy, E-print arXiv:2208.00492.
- , 2023, *GeographicLib, version 2.3*, <https://geographiclib.sourceforge.io/C++/2.3>.
- J. C. Martínez-Llario, S. Baselga, and E. Coll, 2021, *Accurate algorithms for spatial operations on the spheroid in a spatial*

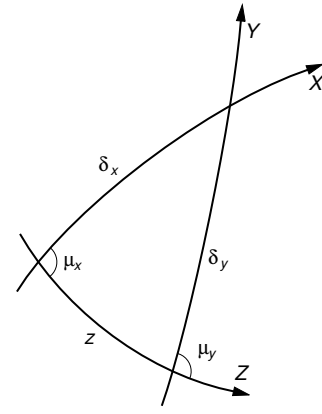


FIG. 7 The spherical trigonometry problem for the basic algorithm.

database management system, Appl. Sci., **11**(11), 5129:1–21, doi:10.3390/app11115129.

L. E. Sjöberg, 2008, *Geodetic intersection on the ellipsoid*, J. Geodesy, **82**(9), 565–567, doi:10.1007/s00190-007-0204-7.

I. Todhunter, 1886, *Spherical Trigonometry* (Macmillan, London), 5th edition, <https://www.gutenberg.org/ebooks/19770>.

Appendix A: The basic algorithm

The core of the algorithm given by *BML* starts with a tentative intersection $\mathbf{S} = [x, y]$ and produces an improved intersection $\mathbf{S}' = [x', y']$. The steps are as follows:

1. Solve the direct geodesic problem for each geodesic to determine (ϕ_x, λ_x) , α_x and (ϕ_y, λ_y) , α_y at the tentative intersection.
2. The geodesic Z connects (ϕ_x, λ_x) and (ϕ_y, λ_y) . Solve the corresponding inverse geodesic problem and find the distance z and the azimuths at the endpoints γ_x and γ_y . (We use γ to denote the azimuths on geodesic Z .)
3. If $z = 0$, set $[\delta_x, \delta_y] = \mathbf{0}$ and go to the last step.
4. The geodesics X , Y , and Z form an ellipsoidal triangle with one edge of length z , and adjacent angles μ_x and $\pi - \mu_y$ where $\mu_x = \gamma_x - \alpha_x$ and $\mu_y = \gamma_y - \alpha_y$; see Fig. 7. The intersection is found by determining the lengths of the other two sides; however, if the triangle is inverted, i.e., $\mu_y - \mu_x \pmod{2\pi} < 0$, first change the signs of μ_x and μ_y .
5. An approximate solution to the ellipsoidal problem is found by solving the corresponding problem on a sphere of radius R ; thus lengths are converted to central angles, for example, by $\zeta = z/R$. The two sides are then given by

$$\frac{\delta_x}{R} = \tan^{-1} \frac{\sin \mu_y \sin \zeta}{\sin \mu_y \cos \mu_x \cos \zeta - \cos \mu_y \sin \mu_x}, \quad (\text{A1})$$

$$\frac{\delta_y}{R} = \tan^{-1} \frac{\sin \mu_x \sin \zeta}{-\sin \mu_x \cos \mu_y \cos \zeta + \cos \mu_x \sin \mu_y}. \quad (\text{A2})$$

6. Set $\mathbf{S}' = \mathbf{S} + [\delta_x, \delta_y]$ as the improved intersection.

These steps define a mapping $\mathbf{S}' = \mathbf{h}(\mathbf{S})$ and this mapping can be repeated to give $\mathbf{S}'' = \mathbf{h}(\mathbf{S}') = \mathbf{h}^2(\mathbf{S})$, $\mathbf{S}''' = \mathbf{h}^3(\mathbf{S})$, etc. In the limit, we have

$$\mathbf{b}(\mathbf{S}) = \lim_{n \rightarrow \infty} \mathbf{h}^n(\mathbf{S}). \quad (\text{A3})$$

This mapping $\mathbf{b}(\mathbf{S})$ constitutes the “basic algorithm”. *BML* apply this starting with the points defining the geodesics, i.e., $\mathbf{S} = \mathbf{0}$, computing $\mathbf{b}(\mathbf{0})$ as the intersection.

A few points require explanation:

- Equations (A1) and (A2), which solve the spherical triangle, are obtained from the cotangent rules given by Todhunter (1886, §44). Superficially they are the same as Eqs. (3) and (4) in *BML*, except that here we ensure that the correct quadrant is chosen for δ_x/R and δ_y/R ; we use the heavy ratio lines in these equations to mean that the quadrant for the arctangent is given by the *separate* signs of the numerator and denominator of the fraction; this functionality is provided by the `atan2` function in many computer languages. This guarantees that δ_x and δ_y are consistent; thus, on the sphere, they advance to the same intersection, and, provided that $\zeta < \pi$, this intersection is the closest.
- Equations (A1) and (A2) are well defined if *either* the numerator or the denominator of the right-hand sides vanishes. However, the equations are indeterminate if *both* the numerator and the denominator vanish, i.e., when $\sin \mu_x \approx \sin \mu_y \approx 0$. This corresponds to *coincident* geodesics X and Y . In this case, a suitable solution is $\delta_x = \frac{1}{2}z \cos \mu_x$ and $\delta_y = -\frac{1}{2}z \cos \mu_y$ which places the intersection midway between the starting points; also set a “coincidence flag”, $c = \pm 1 = \cos \mu_x \cos \mu_y$, to indicate whether the geodesics are parallel or antiparallel. Another case of coincidence is if $\zeta \approx 0$ and $|\sin \mu_x \mp \sin \mu_y| \approx |\cos \mu_x \mp \cos \mu_y| \approx 0$ (i.e., $\mu_y - \mu_x \approx 0$ or π), in which case set the flag $c = \pm 1$. If the geodesics are not coincident, set $c = 0$. A suitable tolerance for the approximate equality here 3ϵ , where ϵ is the precision of the floating-point number system; for standard double-precision arithmetic, we have $\epsilon = 2^{-52}$.
- The algorithm always converges to an intersection, i.e., the limit in Eq. (A3) exists, and the convergence is quadratic. As the algorithm progresses, the sides of the ellipsoidal triangle become shorter and, in the limit, the spherical solution degenerates to the solution for a plane triangle; as a consequence, the quadratic convergence does not depend on the value picked for R . A suitable convergence criterion is $|\delta_x, \delta_y| < \epsilon^{3/4} \pi R$. When this inequality is satisfied, the errors in the updated intersections are, as a result of the quadratic convergence, less than $\epsilon^{3/2} \pi R$, well below the roundoff threshold. Typically about 3 iterations are required for convergence.

Appendix B: Geodesic interceptions

BML also investigate the geodesic interception problem, finding the minimum distance from a point P to a geodesic AB . I give here two improvements to their algorithm. I adopt the notation used by *BML*, who treat A as the tentative interception and compute X , a point on AB as an improved interception. Equation (10) in *BML* can be replaced by

$$\frac{s_{AX}}{R} = \tan^{-1} \frac{\sin(s_{AP}/R) \cos A}{\cos(s_{AP}/R)}, \quad (\text{B1})$$

with the heavy ratio line indicating (as above) that the quadrant is given by the signs of the numerator and denominator, using, for example, the `atan2` function; A is then replaced by X and the process is repeated. A similar formula is given by Martínez-Llario *et al.* (2021), with the caution that it shouldn't be used for $s_{AP}/R \rightarrow \frac{1}{2}\pi$. In fact, this formula is well-behaved in this limit (returning $s_{AX}/R = \pm \frac{1}{2}\pi$ depending on the sign of $\cos A$). Repeated application of Eq. (B1) converges to $\cos A \rightarrow 0$, the condition that the distance from P to the geodesic is an extremum; but, because this equation does not fully capture ellipsoidal effects, the convergence is slower than quadratic. This problem can be corrected using Eq. (B1) for the first iteration and

$$\frac{s_{AX}}{R} = \frac{m_{AP}}{R} \frac{\cos A}{(m_{AP}/s_{AP}) \cos^2 A + M_{AP} \sin^2 A} \quad (\text{B2})$$

for subsequent ones. Here m_{AP} and M_{AP} are the reduced length and geodesic scale for the geodesic connecting A and P , which can be inexpensively computed as part of the geodesic inverse problem (Karney, 2013, §3).

This addresses the core interception problem (the equivalent of the basic algorithm for the intersection problem). Seeking a global optimum solution is bedeviled by the fact that, as shown by Botnev and Ustinov (2015), successive minima in the distance can be arbitrarily close. This is a sharp contrast with the intersection problem where there is a minimum distance between intersections. This problem is addressed by Botnev and Ustinov (2019).